

PAPER • OPEN ACCESS

Finite element design of the connection of barriers for the protection of crowded places

To cite this article: E V Arcieri and S Baragetti 2022 *IOP Conf. Ser.: Mater. Sci. Eng.* **1214** 012028

View the [article online](#) for updates and enhancements.

You may also like

- [Face Detection for Color Image Based on MATLAB](#)
Shahad laith abd al_galib, Asma Abdulelah Abdulrahman and Fouad Shaker Tahir Al-azawi
- [An Enhanced Method for Information Hiding Using LSB Steganography](#)
Mr. Milan Sasmal and Mrs. Debasmita Mula
- [Improving the Lifetime and Cycle Life of NMC/Graphite Li-Ion Cells Charged to 4.4 or 4.5V](#)
Jeff Dahn



The Electrochemical Society
Advancing solid state & electrochemical science & technology

242nd ECS Meeting

Oct 9 – 13, 2022 • Atlanta, GA, US

Abstract submission deadline: **April 8, 2022**

Connect. Engage. Champion. Empower. Accelerate.

MOVE SCIENCE FORWARD



Submit your abstract



Finite element design of the connection of barriers for the protection of crowded places

E V Arcieri and S Baragetti

Department of Management, Information and Production Engineering, University of Bergamo, Viale Marconi 5, Dalmine 24044, Italy

sergio.baragetti@unibg.it

Abstract. The terrorist attacks in Europe have highlighted the problem of safety in public places. It is enough to run a vehicle at high speed towards the crowd to cause a large number of injuries and victims. In response to these phenomena, the Municipalities have perimtered sensitive areas with protection tools. The authors of this work have already designed a mobile anti-terrorism barrier capable of stopping 3500 kg and 7500 kg vehicles with a speed of 64 km/h in a few meters. In this work, the connection of two barriers by ropes is designed using Finite Element (FE) method to perimeter large areas with a small number of devices. Steel and Dyneema® ropes are studied, discussing the number of ropes and the dimensions needed.

1. Introduction

In the recent past, terrorists have wounded and killed many civilians in Nice, Barcelona, London, Stockholm and Berlin by running heavy vehicles at high speed. In response to these attacks, Municipalities have fenced off crowded places such as squares and pedestrian areas, which are sensitive targets for this type of attack.

In general, protection systems can be divided into: (i) fixed, (ii) retractable and (iii) mobile. Fixed systems are very effective although they can be dangerous if impacted by a vehicle because they can be severely damaged and some of their parts can hit people. The presence of foundations requires long installation operations that permanently modify the place where these systems are located and make them expensive. Furthermore, fixed barriers delay rescue operations because they make it difficult for any vehicle to enter the protected areas. Retractable systems (for example mobile bollards) allow the entry of authorized vehicles but they are still expensive because they are equipped with foundation and mechanisms necessary for their movement. Mobile barriers have no foundation and for this reason they can be positioned when and where they are needed and they have a low price. Among the mobile barriers, the most used are the concrete blocks, which dissipate impact energy mainly by friction and are therefore not very effective [1]. Concrete Jersey barriers are commonly adopted to prevent vehicles from entering the opposite lane being more suitable for oblique impacts than for the normal impacts, which can occur in the event of a terrorist attack [2].

The interest in the protection of certain areas is demonstrated by the number of recently designed and patented systems, which exploit different ideas to dissipate the impact energy. In the system presented in [3] part of the impact energy becomes plastic energy. Other energy absorption systems are described in [4] and in [5]. The barrier in [4] can be used as street furniture thanks to its good looks. Another patented solution presents a crash cushion that collapses when the applied axial force is greater



than a threshold [6]. A kind of leverage is shown in [7]: this system raises the vehicle by changing the direction of the vehicle's momentum.

In this scenario, the authors' research group designed in collaboration with Besenconi Defence & Protection S.r.l. and Besenconi S.p.A. a new mobile barrier which is able to stop a 3500 kg van running at 64 km/h in less than 5 m. Thanks to this outstanding result, obtained experimentally, the barrier has been certified [1]. This system also has an aesthetic appeal, which avoids generating a sense of danger in pedestrians. The final shape of the barrier was defined thanks to mathematical and FE modelling and experimental testing [1,8-9]. FE method was also adopted to demonstrate the effectiveness of a single barrier in stopping a 7500 kg truck travelling at 64 km/h [10]. However, Municipalities should protect large areas using a limited number of barriers. In this work, conducted in collaboration with Besenconi Defence & Protection S.r.l. and Besenconi S.p.A., the connection of two barriers is designed using FE method. Steel and Dyneema® [11] ropes are arranged in different configurations, assessing each time the loads involved.

2. Materials and methods

This work deals with the design of the connection between two barriers of the type described in [1,8,10]. The designed barrier, shown in Figure 1, is mobile and it is good looking, so it can be used as street furniture. It consists of a cast iron base and several steel perimeter sheets. In [1] the use of aluminium was investigated as a consequence of the research group expertise in its alloys [12-13]. Any treatments such as the deposition of coatings [14-15] were not considered. The dimensions are 3000 mm x 860 mm x 1010 mm and the mass is approximately 2050 kg. In the barrier there is a bag containing 1550 kg of water, with different purposes: (i) the water allows to reach a significant mass, useful for dissipation by friction, after positioning the barrier so the transport of the system is facilitated; (ii) the release of large amounts of water following the impact takes away a lot of energy. The plastic strain of the barrier contributes to the dissipation of the impact energy [1,8-10].

The modelling techniques described in [10] were adopted for the purpose of this paper. FE analysis was conducted with Abaqus/Explicit 6.14-5, as explicit integration methods are suitable for impacts [16-18]. The behavior of the water contained in the barrier was studied using a Smoothed Particle Hydrodynamics approach [19].

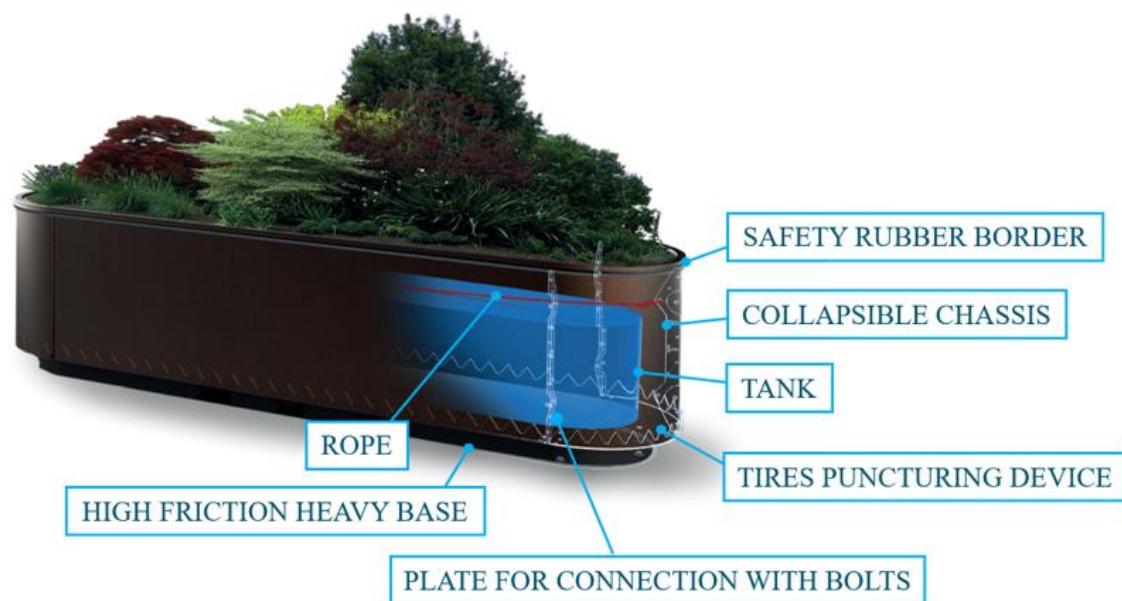


Figure 1. Barrier [1,8,10].

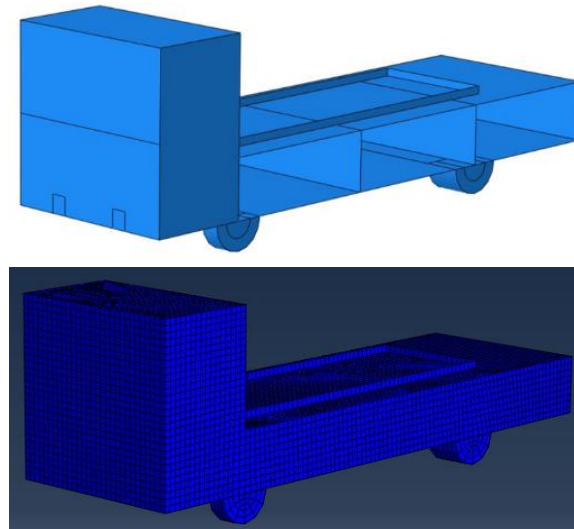
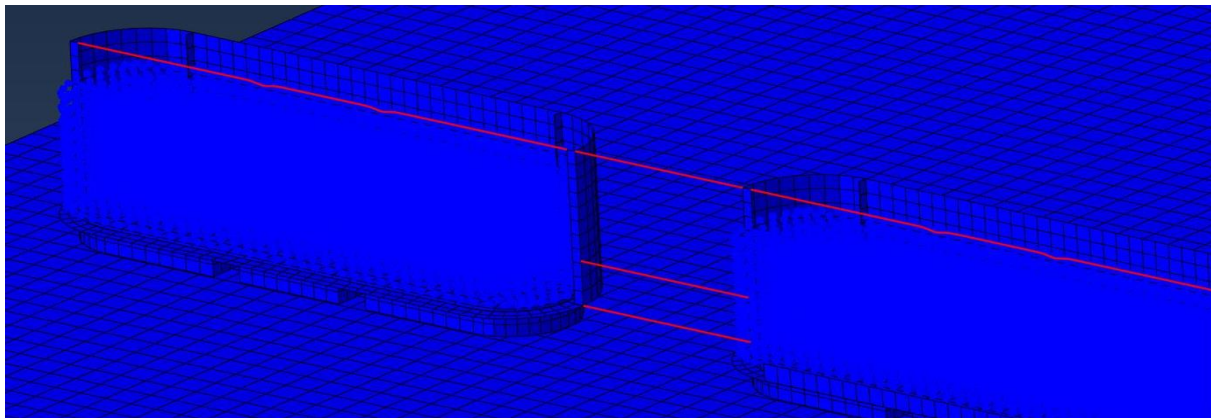


Figure 2. Model of the vehicle: geometry and mesh [10].

The normal impact of an Iveco Eurocargo ML120E24 against the center of the system consisting of two connected barriers was studied. The vehicle data are as follows: wheelbase 4185 mm; mass 7500 kg with ballast; height from the ground 358 mm at the front; position of the center of gravity in longitudinal direction 1785 mm from the front axle; vertical position of the center of gravity 970 mm above the ground [20]. The truck was modelled as two parallelepipeds of shell elements with suitable width (6 or 8 mm) and a frame of shell elements on the bodywork reproducing the ballast. The truck was stiffened to have 20% deformability and two side members and two cross members were inserted to reduce surface bending as visible in Figure 2 [10], where some surfaces are removed to show the inner part. The lack of experimental results makes the authors assume a linear elastic material behavior for the wheels. According to this hypothesis, they resist impact. Table 1 shows the materials of the FE model. For each of them it is indicated which component it is assigned to and what its properties are [8,10,21-22]. The steel properties were also assigned to the vehicle surfaces, although the density value was changed to ensure the correct position of the vehicle's center of gravity. For water, the Wilkins energy equation [23] was adopted and for this reason the reference sound speed is indicated in Table 1 [8,10,21-22]. It was decided to connect the barriers with ropes. In [24] a theoretical model for the nonlinear bending of wires is proposed. For them, an indefinite elastic behavior was conservatively assumed with attention not to exceed the limit load during the simulation since exceeding this value would imply the failure of the connection in reality. The ropes were modeled with truss elements of circular section. It was assumed the use of two types of materials: steel and Dyneema®. Dyneema® is particularly suitable for traction cables and it consists of a synthetic fiber of high-strength polyethylene with very high molecular weight and extremely long molecules that allow the force to be transferred much more effectively. In terms of resistance, Dyneema® ropes are comparable to steel ropes with the advantage of not being subject to corrosion problems. They are also able to withstand the ultraviolet rays and through experimental tests this material has shown good resistance to fire [22,25]. The last property is very important because it prevents that someone burns the ropes making ineffective the system. Corrosion resistance is another important aspect in a huge variety of applications [26-27]. The ropes were positioned at different heights and connected to the vertical edges of the barrier by coupling type connections. Kinematic connections were used for the coupling of the perimeter sheets. The friction behavior in threaded connections [28] was not implemented. The ground was modelled as a surface of shell elements with high stiffness and the nodes fixed in order to avoid the deformation of the ground.

Table 1. Materials [8,10,21-22].

Material	Assigned to	Density (kg/m ³)	Young's modulus (MPa)	Poisson's ratio	Yield stress (MPa)	Reference sound speed (m/s)
S235JR (Elastic-perfectly plastic)	Perimeter sheets Vehicle (Different density)	7800	206000	0.30	235	
Cast iron (Elastic-perfectly plastic)	Base	7300	120000	0.26	250	
Water	Fluid	1000				1450
Rope (Steel - elastic)	Ropes	7800	110000	0.30		
Rope (Dyneema® – elastic)	Ropes	3000	132000	0.30		

**Figure 3.** Three connecting ropes and one internal rope in Dyneema®: arrangement of the ropes.

The FE analyzes performed consist of a first calculation step of 20 ms and a second one of 400 ms: in the first one, the gravitational load applied made the components come into contact; in the second, the impact between the truck and the obstacle was simulated. The pieces of the barrier and the vehicle were joined by means of constraints. In order to prevent all parts from interpenetrating, frictionless general contact was implemented throughout the model. The interactions with the friction coefficients of [10] were implemented to define the behavior between some regions of the model. In the model, the wheels cannot rotate in order to reduce the computational cost. To simulate the rolling friction, a coefficient of friction of 0.01 was implemented between the ground and the wheels.

3. Results and discussion

3.1. Three connecting ropes and one internal rope in Dyneema®

The first case analyzed refers to the impact of a 7500 kg vehicle running at 64 km/h against two barriers placed at a distance of 1 m from each other and connected by Dyneema® ropes with a diameter of 20 mm. The limit load for these ropes is 230 kN [29]. Three ropes were placed at 1 m (C1), 0.39 m (C2) and 0.13 m (C3) from the ground (Figure 3). A rope was inserted into each barrier to make the part of the barrier far from the impact zone cooperate in absorbing the impact energy. The internal ropes, I1 and I2, were inserted in the upper part, coaxial to the rope C1. In this case of connection between two barriers, the 7500 kg vehicle was stopped in 3 m. The following maximum axial loads were obtained: 183 kN for C1, 17 kN for C2, 3 kN for C3, 60 kN for I1 and 51 kN for I2. C3 is the most loaded rope and all the loads are below the limit so the ropes resist. The results are quite symmetric. Even if the

model mesh was as symmetric as possible and symmetry conditions were implemented, the complexity of the problem analyzed may be responsible for this behavior. The lack of perfect symmetry overloaded a rope rather than the symmetric one. It is reasonable to suppose that in a condition of perfect symmetry the load on the two ropes would be intermediate. Since the study conducted focused on the maximum values of load obtained for the ropes, it was precautionary. Furthermore, it is difficult for a perfectly symmetric situation to occur in reality.

In addition to the analysis of the loads on the ropes, the equivalent plastic deformation (PEEQ) of the sheets after impact was also analyzed. It can be estimated that the failure of the barrier sheets occurs in those areas where the PEEQ is greater than the elongation A% of the material. In the case of S235JR steel, which is the material of the sheets, this value is 0.26 [30]. Figure 4 shows the PEEQ field for the analyzed case. By setting A% = 0.26 as the upper limit of the chromatic scale, it is possible to identify the points that exceed A%, which are the gray areas. For this first case of analysis, it can be noted in Figure 4 that these areas correspond to the impact areas and those of attachment of the ropes. The failure of these areas is useful for dissipating part of the impact energy and therefore for stopping the vehicle.

3.2. Three connecting ropes and two internal ropes in steel

Starting with the model presented in Section 3.1, one internal rope was added for each barrier, coaxial to C2. These two additional ropes are called I3 and I4 in this manuscript with I3 under I1 and I4 under I2. 16 mm steel ropes were still implemented. The stopping distance in this case is 5 m. The following loads were obtained: 168 kN for C1, 4 kN for C2, 2 kN for C3, 69 kN for I1, 46 kN for I2, 20 kN for I3 and 15 kN for I4. The C1 rope is the one that basically works among the connecting ones. The PEEQ distribution shown in Figure 5 was obtained. The position of the gray areas is similar to that of the previous cases. In summary, this configuration presents an improvement in terms of load on the connecting ropes compared to previous models, especially for the middle and lower ropes. However, in parallel with the decrease in the load on the connecting ropes, an increase in displacement of 2 m was obtained compared to the models with only one internal rope. This decrease in performance is attributable to the increased rigidity of the system due to the presence of a greater number of ropes. It was therefore decided to no longer analyze the insertion of a second internal rope in each barrier. The presence of this rope would also complicate the assembling of the single barrier as it would interfere with the water tank inside.

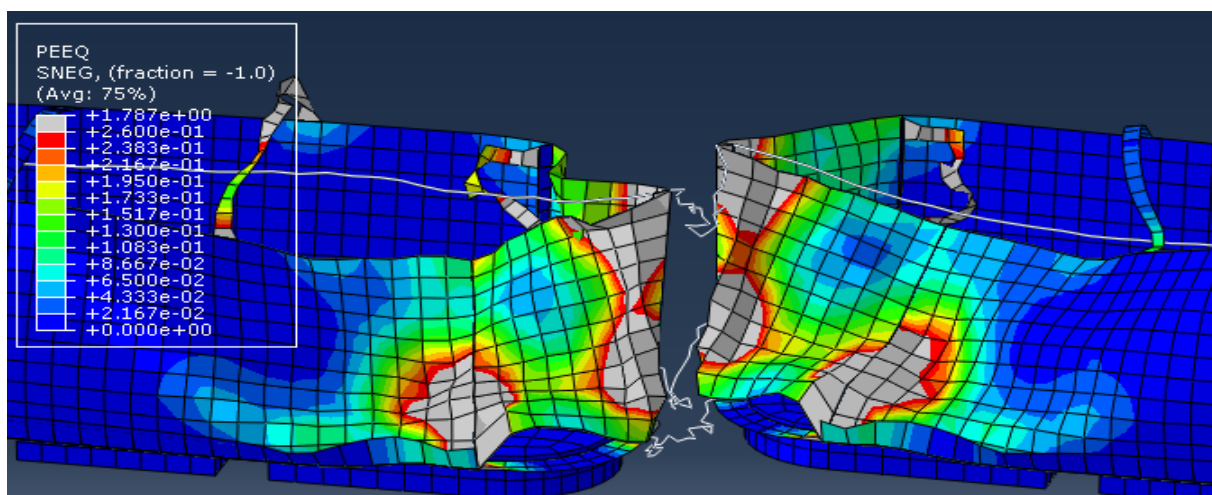


Figure 4. Three connecting ropes and one internal rope in Dyneema®: PEEQ.

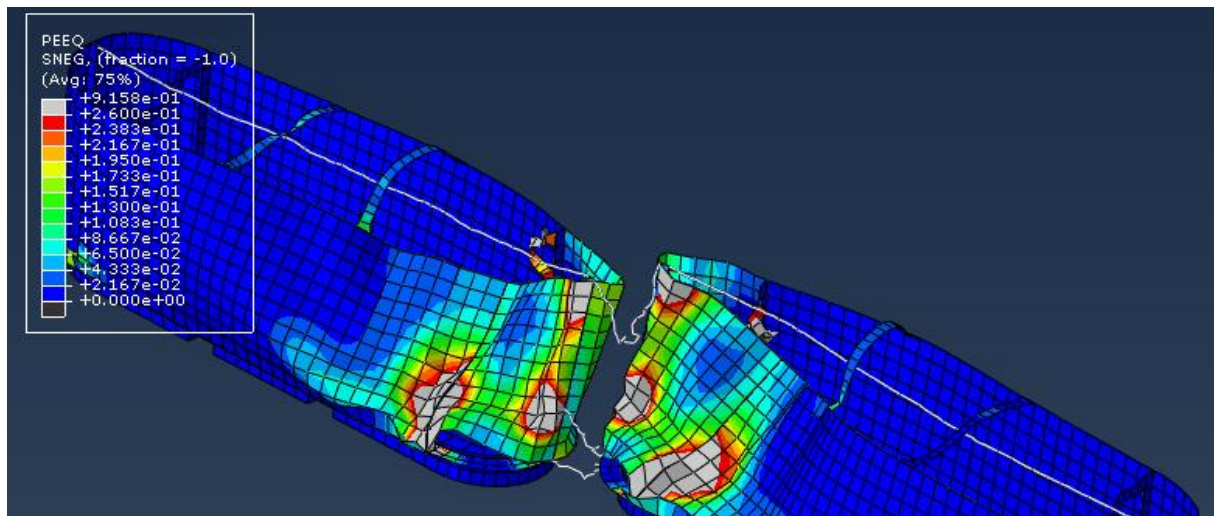


Figure 5. Three connecting ropes and two internal ropes in steel: PEEQ.

3.3. One connecting rope and one internal rope in Dyneema®

Analysing the stress state in the ropes of Sections 3.1 and 3.2 it was noted that the connecting ropes C2 and C3 were almost unloaded. It was therefore decided to keep only C1 as a connecting rope. A 60 mm diameter rope in Dyneema® was chosen. The internal ropes, on the other hand, still had a diameter of 20 mm. To identify the limiting load for the 60 mm rope, extrapolation from the data in [29] was carried out which gave a limiting load of 730 kN. Figure 6 shows the FE model of the new configuration. The following loads are obtained on the ropes: 152 kN on C1, 53 kN on I1 and 27 kN on I2. According to the results, all the ropes would resist. Analysing the PEEQ values in Figure 7, at the end of the simulation, it can be seen that the extension of the areas that exceed the percentage of elongation A% is greater. In fact, during the impact dynamics the barriers tend to get closer to each other. This behaviour is due to a greater axial stiffness of the rope, associated with the increase in the diameter of the rope. The rope, if subject to traction, attracts with greater force the barriers to which it is connected. The possible tearing of the sheets can be a favourable effect as it dissipates a part of the impact energy. In order to reduce the failure, reinforcements could be positioned in these areas. A displacement of 3 m was obtained. A configuration of this type is therefore adequate both in terms of construction and performance obtained. It is possible to replace the ropes with chains of similar properties.

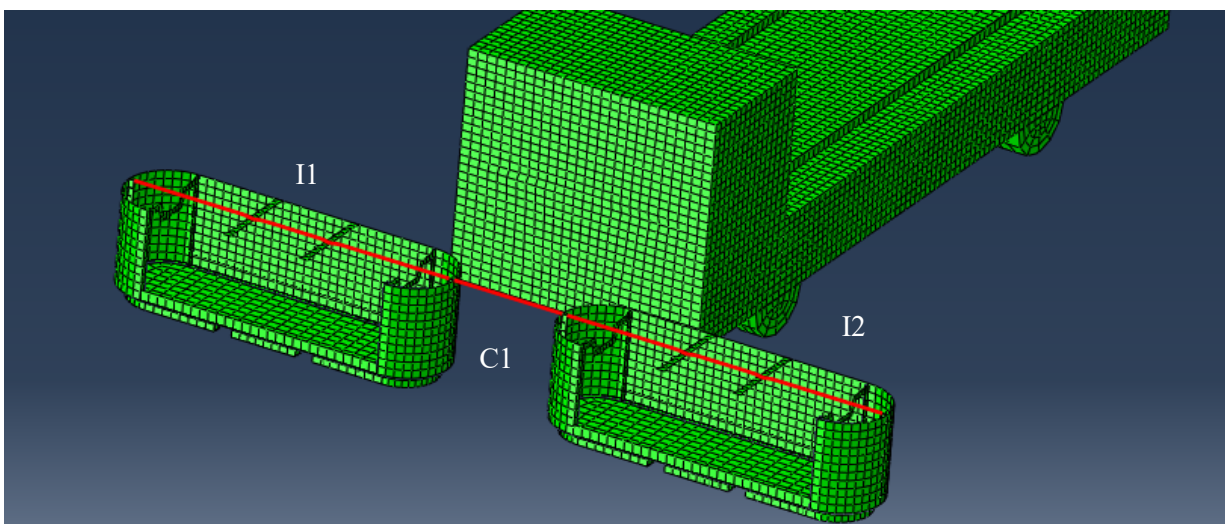


Figure 6. One connecting rope and one internal rope in Dyneema®: model.

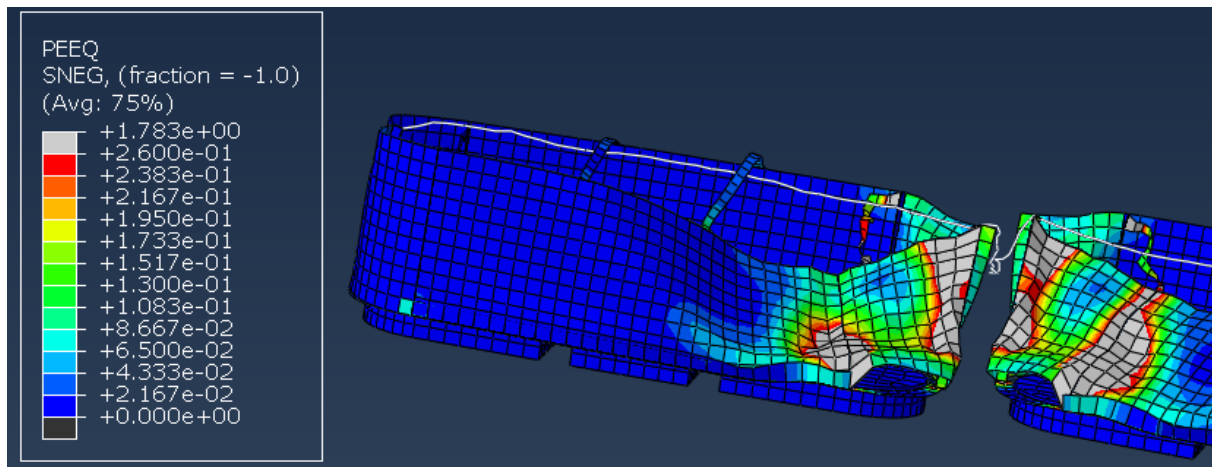


Figure 7. One connecting rope and one internal rope in steel: PEEQ.

4. Conclusions

The terrorist attacks in Europe have highlighted the issue of safety in public places. It is enough to run a vehicle at high speed towards the crowd to cause a large number of injuries and victims. The authors of this work have already designed a mobile anti-terrorism barrier capable of stopping 3500 kg and 7500 kg vehicles running at 64 km/h in a few meters. In this work, the connection of two barriers is designed using the FE method to perimeter large areas with a small number of devices. Three configurations are studied, evaluating each time the loads involved in the case of the normal collision of a truck. It was chosen a configuration consisting of the two barriers at a distance of 1 m connected by a Dyneema® rope with a diameter of 60 mm and with a coaxial internal rope with a diameter of 20 mm. As failure was not implemented in the model, the PEEQ analysis revealed which areas of the barrier could actually be damaged. They coincide with the areas where the impact occurs and where the ropes are connected. The failure of the barrier sheets could be a good effect, as it dissipates some of the impact energy.

Acknowledgments

The authors would like to thank Besenzoni Defence & Protection S.r.l., Besenzoni S.p.A., Federico Locatelli and Alessandro Sala for their support in the work.

References

- [1] Baragetti S and Arcieri E V 2019 Proc. *ASME Int. Mechanical Engineering Congr. and Expo.* vol 14 (Salt Lake City) 156960
- [2] Kala J, Hradil P and Salajka V 2012 *Int. J. Civ. Eng.* **6** 831
- [3] Amengual Pericas A 2009 Patent EP2314772B1
- [4] Shen L, Caspe M, Ji J and Wang Q 2010 Proc. *Building Design + Construction*
- [5] Stevanato A 2014 Patent US2017362788
- [6] Impero P 2013 Patent ZA201507239
- [7] <https://barriers.miframsecurity.com/products/mvb-3x/>. [Accessed on 12/01/2019]
- [8] Baragetti S and Arcieri E V 2019 *Procedia Struct. Integrity* **24** 91
- [9] Baragetti S and Arcieri E V 2020 *Eng. Fail. Anal.* **113** 104564
- [10] Arcieri E V and Baragetti S 2021 *IOP Conf. Ser.: Mater. Sci. Eng.* **1038** 012008
- [11] https://www.dsm.com/dyneema/en_GB/home.html [Accessed on 03/12/2019]
- [12] Baragetti S and D'Urso G 2014 *J. Mech. Sci. Technol.* **28** 867
- [13] Baragetti S and Arcieri E V 2020 Proc. *Inst. Mech. Eng. Part C J. Mech. Eng. Sci.* online
- [14] Baragetti S, Gelfi M, La Vecchia G M and Lecis N 2005 *Fatigue Fract. Eng. Mater. Struct.* **28** 615
- [15] Baragetti S and Tordini F 2007 *Int. J. Fatigue* **29** 1832

- [16] Arcieri E V, Baragetti S, Fustinoni M, Lanzini S and Papalia R 2018 *Procedia Struct. Integrity* **8** 212
- [17] Baragetti S, Guagliano M and Vergani L 2000 *J. Mech. Sci. Product. Technol.* **15** 91
- [18] Arcieri E V, Baragetti S and Lavella M 2021 *IOP Conf. Ser.: Mater. Sci. Eng.* **1038** 012012
- [19] Monaghan J J 2005 *Rep. Prog. Phys.* **68** 1703-1759
- [20] https://private.iveco.com/italy/collections/technical_sheets/Documents/usato/medi/medium%202/ML120E24FP.pdf [Accessed on 01/10/2018]
- [21] <http://www.teci.it/funi/standard-a-trefoli/s10-zn-s11-zn/> [Accessed on 03/12/2019]
- [22] <https://www.xvertical.it/dyneema-e-kevlar/> [Accessed on 03/12/2019]
- [23] Wilkins M L 1999 *Computer Simulation of Dynamic Phenomena* (Berlin: Springer-Verlag Berlin Heidelberg)
- [24] Baragetti S 2006 *Meccanica* **41** 443
- [25] Locatelli F and Sala A 2019 *Modellazione numerica esplicita e implicita di strutture innovative per la sicurezza e il settore nautico: modelli teorici, numerici e riscontri sperimentali* master thesis
- [26] Baragetti S 2013 *Surf. Interface Anal.* **45** 1654
- [27] Baragetti S and Arcieri E V 2018 *Int. J. Fatigue* **112** 301
- [28] Baragetti S, Terranova A and Vimercati M 2009 *Int. J. Mech. Sci.* **51** 790
- [29] <https://www.armare.it/it/>. [Accessed on 03/12/2019]
- [30] <https://irp-cdn.multiscreensite.com/057cab6f/docs/1.3716043..pdf> [Accessed on 03/12/2019]